REVIEW

Intracranial 3D and 4D MR Angiography Using Arterial Spin Labeling: Technical Considerations

Yuriko Suzuki[1*], Noriyuki Fujima[2], and Matthias J.P. van Osch[3]

In the 1980's some of the earliest studies of arterial spin labeling (ASL) MRI have demonstrated its ability to generate MR angiography (MRA) images. Thanks to many technical improvements, ASL has been successfully moving its position from the realm of research into the clinical area, albeit more known as perfusion imaging than as MRA. For MRA imaging, other techniques such as time-of-flight, phase contrast MRA and contrast-enhanced (CE) MRA are more popular choices for clinical applications. In the last decade, however, ASL-MRA has been experiencing a remarkable revival, especially because of its non-invasive nature, i.e. the fact that it does not rely on the use of contrast agent. Very importantly, there are additional benefits of using ASL for MRA. For example, its higher flexibility to achieve both high spatial and temporal resolution than CE dynamic MRA, and the capability of vessel specific visualization, in which the vascular tree arising from a selected artery can be exclusively visualized. In this article, the implementation and recent developments of ASL-based MRA are discussed; not only focusing on the basic sequences based upon pulsed ASL or pseudo-continuous ASL, but also including more recent labeling approaches, such as vessel-selective labeling, velocity-selective ASL, vessel-encoded ASL and time-encoded ASL. Although these ASL techniques have been already utilized in perfusion imaging and their usefulness has been suggested by many studies, some additional considerations should be made when employing them for MRA, since there is something more than the difference of the spatial resolution of the readout sequence. Moreover, extensive discussion is included on what readout sequence to use, especially by highlighting how to achieve high spatial resolution while keeping scan-time reasonable such that the ASL-MRA sequence can easily be included into a clinical examination.

Keywords: *arterial spin labeling (ASL), dynamic MR angiography, non-contrast enhanced MR angiography, vessel-selective MR angiography*

Introduction

For many cerebrovascular diseases, visualization of blood flow through the large vasculature and microvascular information of downstream brain tissue can be crucial for diagnosis and monitoring of disease progression and treatment efficacy. The former is achieved by angiography and the latter is assessed by perfusion imaging; both can be obtained by means of arterial spin labeling (ASL) techniques. In ASL,

the visualization of arterial flow is achieved by labeling the magnetization of arterial blood using radiofrequency (RF) pulses, which allows the labeled blood to act as an endogenous tracer, thereby eliminating reliance on the use of contrast agents. By taking advantage of this completely non-invasive feature, many studies were conducted to demonstrate that ASL can be an alternative technique for other more invasive techniques using X-ray and/or contrast agent.[1–7] This would especially be important for pediatric patients who need repetitive examinations to monitor disease progression. Whereas MR contrast agents used to be considered relatively safe, due to the established link between several linear gadolinium contrast agents and nephrogenic systemic fibrosis in patients with poor renal function as well as the recent observation of gadolinium deposition in the brain,[8] the European Medicines Agency decided to recommend the suspension of the use of four linear MR contrast agents and advise to limit the use of gadolinium based contrast agents to the lowest dose for diagnosis. It is clear that

[1]Institute of Biomedical Engineering, University of Oxford, Oxford, UK
[2]Department of Diagnostic and Interventional Radiology, Hokkaido University Hospital, Hokkaido, Japan
[3]Department of Radiology, Leiden University Medical Center, Leiden, The Netherlands

*Corresponding author: Institute of Biomedical Engineering, University of Oxford, Oxford, UK. E-mail: yuriko.suzuki@eng.ox.ac.uk

there is an urgent reason to pursue the establishment of non-contrast-enhanced (non-CE) examination. In 2015, a statement for recommended implementation of ASL for clinical perfusion imaging was published by the perfusion study group of the International Society for Magnetic Resonance in Medicine (ISMRM) and European Cooperation in Science and Technology (EU-COST) action "ASL in dementia", which suggests that ASL perfusion MRI has become ready for clinical use.[9]

Although less widespread than ASL perfusion imaging, the use of ASL technique for MR angiography (MRA) has also been getting more attention recently, especially for applications in the brain. Even apart from the ability to visualize arterial flow without using the contrast agent, there are considerable advantages of ASL-based MRA over other MRA techniques such as time-of-flight (TOF) MRA and dynamic CE-MRA. First, in dynamic CE-MRA, the first passage of the contrast agent bolus needs to be captured by a real-time dynamic acquisition. Due to very fast passage of the contrast agent through the vascular tree and the early appearance of venous signal, each dynamic must be acquired very quickly, therefore, the spatial resolution is often compromised. Although highly undersampled non-Cartesian acquisitions and several elaborate reconstruction techniques have been proposed to alleviate some of these limitations,[10–15] not all those techniques are already available in clinical setting. In ASL, on the other hand, it is not necessary to acquire all data during a single bolus passage, therefore, both high spatial and temporal resolution can be achieved by repeating the labeling of the arterial blood and following data acquisition. The typical temporal resolution in ASL-based dynamic 3D-MRA (referred to as "4D-MRA") is 100–200 ms, which is much higher than for dynamic CE-MRA. Such high temporal resolution can be very important, especially when evaluating arteriovenous shunts. In Fig. 1, for example, TOF-MRA images show abnormally dilated arterial brunches and enhanced sinuses, which suggest a dural arteriovenous fistula fed mainly by the right occipital artery. Additionally, ASL-based 4D-MRA images acquired with a temporal resolution of about 200 ms successfully visualized that the labeled arterial blood is flowing into the sinuses retrogradely (indicated by arrows in Fig. 1). It can be speculated that such retrograde flow into the sinuses will continue into the cortical vein, which is significantly related to a high incidence of hemorrhage.

The second advantage of ASL-MRA is the ability to achieve vessel specific visualization, in which the vascular tree originating from a selected artery can be exclusively visualized by spatially selective labeling. Figure 2 shows an example of how vessel-selective ASL-MRA is applied to a clinical case of an arteriovenous malformation (AVM).[16] Whereas TOF-MRA visualizes the large nidus very clearly, vessel-selective ASL-MRA is providing additional information by showing which arteries are responsible for feeding the nidus. Such information could be useful for pre-operative
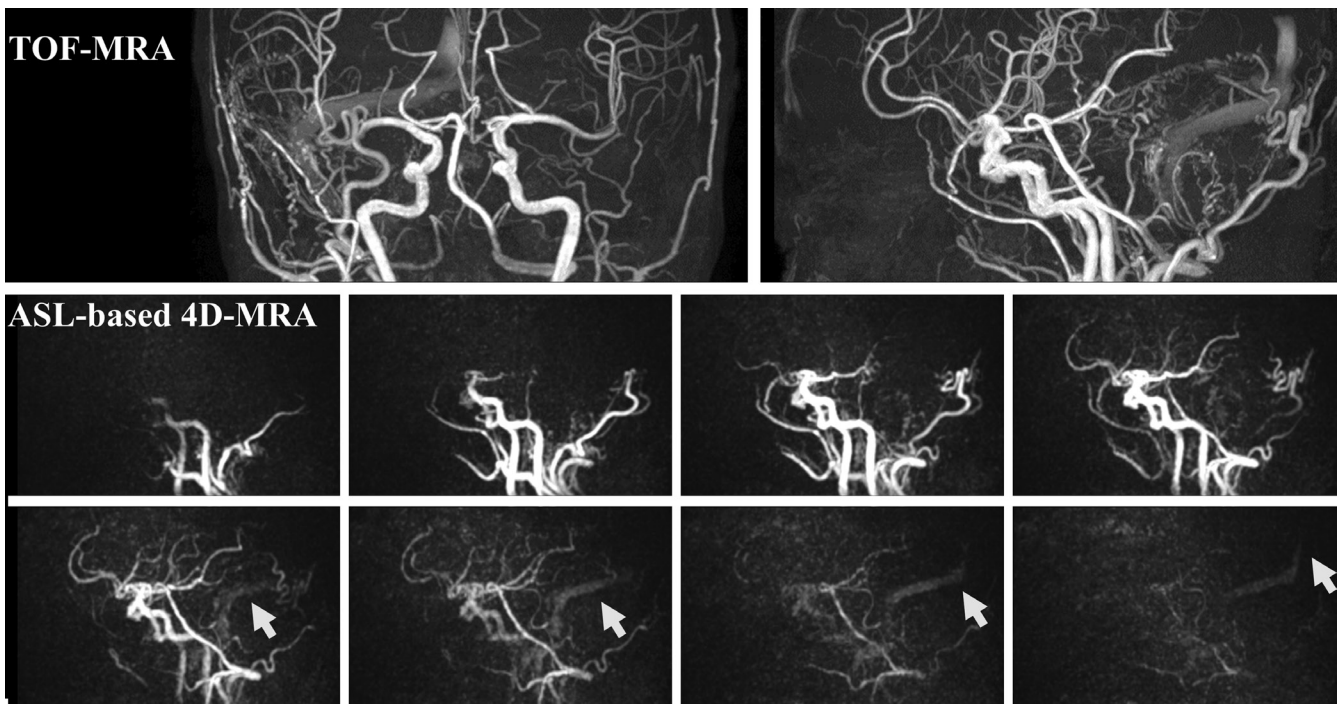

Fig. 1 TOF-MRA images show abnormally dilated arterial brunches and enhanced sinuses, which suggest a dural arteriovenous fistula fed mainly by the right occipital artery. Additionally, ASL-based 4D-MRA images successfully visualized that the labeled arterial blood is flowing into the sinuses retrogradely (indicated by arrows). The temporal resolution of 4D-MRA is about 200 ms. TOF, time-of-flight; ASL, arterial spin labeling; MRA, magnetic resonance angiography.
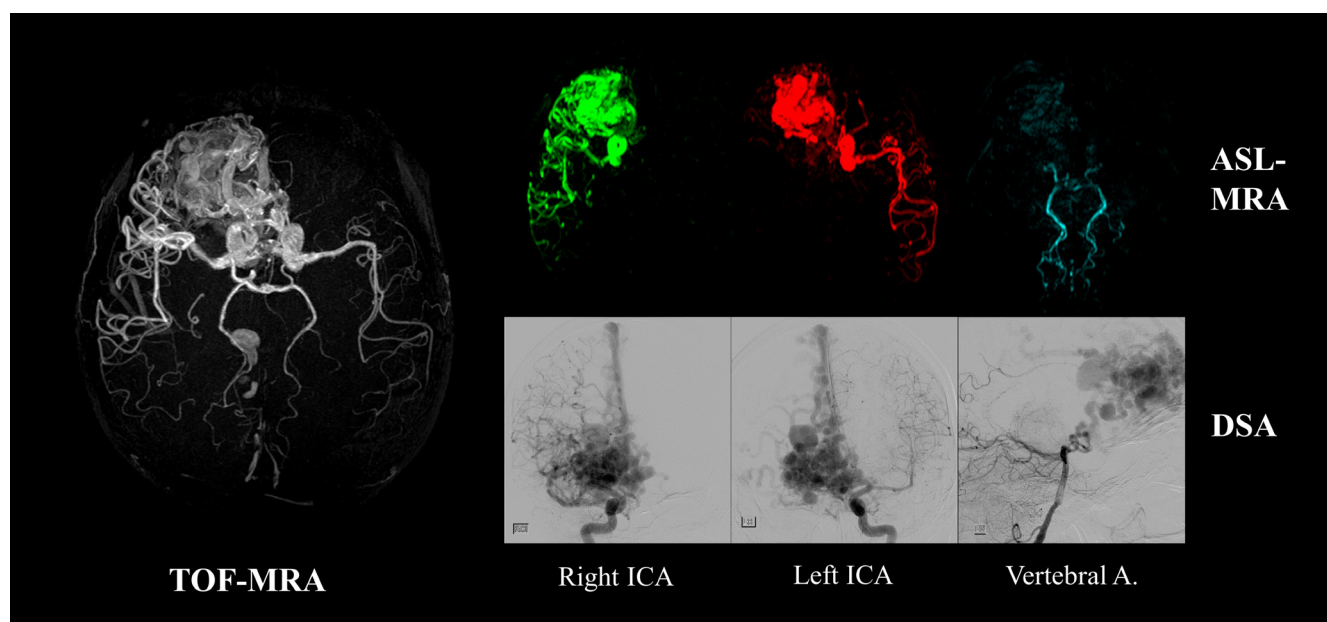
Fig. 2 A clinical example of vessel-selective 3D arterial spin labeling-MR angiography (ASL-MRA) applied to an arteriovenous malformation. Whereas TOF-MRA visualizes the large nidus very clearly, vessel-selective ASL-MRA shows which arteries are feeding the nidus. Image were reproduced from Jensen-Kondering et al.[16] with permission from Dr. Michael Helle, Philips GmbH Innovative Technologies. TOF, time-of-flight; ICA, internal carotid artery.

preparations for X-ray digital subtraction angiography (DSA), or could even be a potential alternative to X-ray DSA as a follow-up examination.

Additionally, it should be also noted that, in dynamic CE-MRA and X-ray DSA, the contrast agent will be injected using a power-injector at a high-speed, which may cause an altered blood flow from the normal physiological condition.[17] In contrast, the information obtained by ASL-based 4D-MRA potentially reflects the natural physiological blood flow condition.

In this article, the implementation and recent developments of ASL-based MRA will be reviewed. Although one may naively assume that "just replacing the readout of an ASL perfusion imaging by a 3D high-resolution sequence" would be all to say, there are several important considerations before "just" changing the readout sequence. Since ASL techniques have already been used widely for perfusion imaging, this review article will mainly focus on the technical differences between ASL-MRA and ASL perfusion imaging, which were selected from the list of PubMed search with the keywords of "Arterial Spin Labeling" and "Angiography (MRA)". Additionally, articles describing clinical applications using ASL-based MRA were reviewed. More detailed description about the principles of ASL can be found in several excellent review articles.[18–21]

Spatial Resolution and Readout Sequence

As mentioned above, the most obvious difference between the acquisition of ASL-MRA and ASL perfusion image is the spatial resolution of the readout sequence, which is a consequence of the expected ASL-signal produced by the labeled spins for each image type. In perfusion imaging, the ASL-signal produced by the labeled spins that traveled all the way from the labeling plane to the brain tissue is very small, typically <1–2% of the gray matter signal, which can be calculated from the cerebral blood flow (CBF) (i.e. a CBF-value of 60 mL/min/100 mL implies that, in a minute, arterial blood that would flow into a voxel is equivalent to 60% of the voxel-volume, which means that when labeling is applied for 2 s, arterial blood equivalent to only 2% of the voxel-volume would enter the voxel) and T_1-relaxation of the labeled spins. Because such subtle signal differences have to be visualized, the readout is performed with large voxel-sizes of typically 3–4 mm in-plane and 3–8 mm through-plane (or iso-voxel for 3D-readout).[9] Moreover, this is combined with repeated signal averaging to further leverage the signal-to-noise ratio (SNR). For MRA, in contrast, much stronger ASL-signal will be measured within the arterial vessels, because the complete lumen is filled by labeled spins, and data is usually acquired at much shorter delay time (inversion-time; TI or post-labeling delay; PLD), i.e. less T_1-relaxation. Therefore, a 3D-readout with much smaller voxel-size is used, which is also required to depict smaller arteries. Although the ideal spatial resolution has not been standardized yet, the voxel-sizes from previous studies are typically 1.0–1.25 mm in in-plane and 1.0–2.0 mm in through-plane direction (potentially reconstructed at even higher resolution).[1,4,22–24] Therefore, the entire scan-time usually needs to be spent for completing k-space, not for signal averaging as in perfusion imaging.
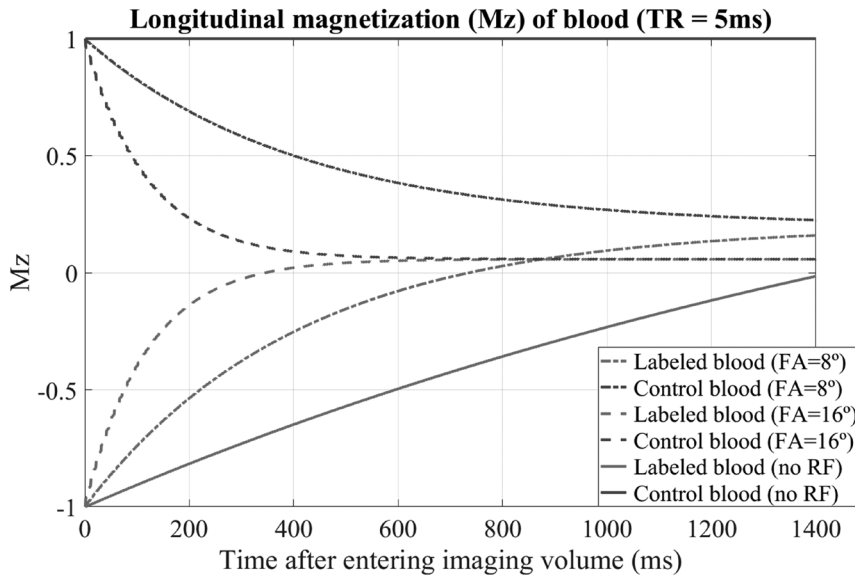
Fig. 3 The behavior of the longitudinal magnetization (M_z) was simulated by means of Bloch equation simulations, by assuming the labeled blood (in labeling image) and non-labeled blood (in control image) enter the imaging volume and receive excitation RF-pulses over 1400 ms. The transverse magnetization was assumed to be spoiled before the next excitation pulse is applied. The T_1 and T_2 of blood were assumed to be 1650 ms[9] and 150 ms,[78] respectively. RF, radiofrequency; FA, flip-angle.

The typical readout sequence used for ASL-MRA is based on gradient-echo sequences, such as turbo field-echo (TFE)[2,3] and spoiled gradient-echo (SPGR),[24–27] in which quite a number of excitation RF-pulses are applied. For dynamic MRA, the acquisition of multiple TIs/PLDs is generally performed using a Look-Locker readout,[28] in which the gradient-echo sequence is segmented into shorter shots with a duration equal to (or shorter than) the desired temporal resolution (typically 100–200 ms). Subsequently, the same k-space lines are repeatedly acquired to obtain images with different TIs/PLDs. However, this also implies that the blood spins will receive even more RF-pulses once the labeled blood has entered the imaging volume. Therefore, it is important to consider how those RF-pulses will affect ASL-signal.

In ASL-MRA, the control image will show the arterial blood signal with high intensity (like TOF-MRA), while the labeled blood will have negative or small signal, and the difference between these two states constitutes the ASL-signal. Therefore, both obtaining high arterial blood signal in the control image and maintaining the label in the labeling image is important to generate strong ASL-signal in the arteries. Importantly, excitation RF-pulses applied in the readout sequence will saturate the arterial signal in the control image (again just same as TOF-MRA), while T_1-relaxation of the labeled magnetization is accelerated by the same RF-pulses (Fig. 3). Taken both effects together makes clear that ASL-signal in the subtracted angiographic image will be also decreased. This attenuation will especially be problematic in later phases of dynamic acquisition. To preserve as much as magnetization for later phases, rather low excitation flip-angle (FA) (typically 6–10°) is used compromising overall signal intensity.

This attenuation of ASL-signal can be alleviated by reducing the number of RF-pulses by acquiring more than one k-line per excitation pulse by e.g. using echo planar
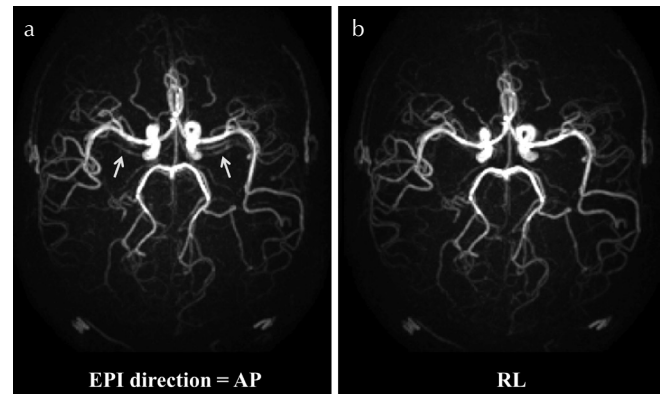

Fig. 4 ASL-MRA obtained by TFEPI sequence. Typical ghosting artefacts due to pulsatile flow is shown in (**a**) when the phase-encoding direction is set in the anterior–posterior (AP) direction (see arrows). By changing the phase-encoding to the right–left (RL) direction, the artefacts were substantially reduced (**b**). ASL-MRA, arterial spin labeling-magnetic resonance angiography; TFEPI, turbo field echo planar imaging.

imaging (EPI) readout. In a turbo field EPI (TFEPI) sequence,[29] a segmented EPI readout (with typical EPI-factor of 5–7[4,30,31]) is performed after each excitation pulse of the TFE sequence to reduce the number of excitation RF-pulse, thereby limiting the attenuation of the ASL-signal. The downside of inserting an EPI readout is that it causes ghosting artefacts due to pulsatile flow, which happens more frequently in young subjects, typically at the M1 section of the middle cerebral artery (arrows in Fig. 4a). In many cases, however, setting the phase-encoding direction to the right–left direction (instead of the anterior-posterior direction) helps to reduce the apparent artefacts (Fig. 4b).

Another option is balanced steady-state free precession (bSSFP) sequence,[22,32,33] in which the transverse magnetization is recycled for the next TR without being spoiled,
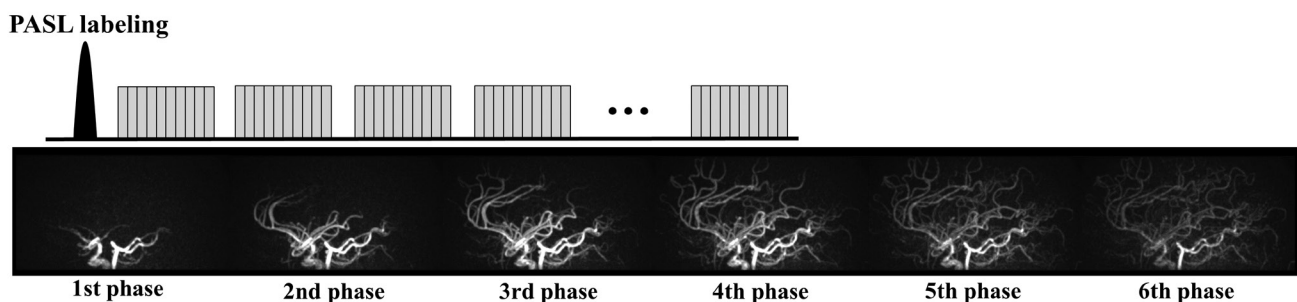
thereby alleviating both the saturation of arterial blood in the control image and the acceleration of T_1-relaxation of the labeled blood in the labeling image. In a previous study by Okell et al.,[32] the behavior of the magnetization with several scenarios was simulated, e.g.: (i) bSSFP sequence with TR of 4.2 ms and excitation FA of 40° and (ii) SPGR sequence with TR of 12.0 ms and FA of 8°. Please note that the scan-time of scenario-(i) will be much shorter than (ii) due to shorter TR. The results showed that the longitudinal magnetization of (i) and (ii) behaved very similarly over 1000 ms readout duration even though much shorter TR and higher FA were used in scenario-(i). Moreover, much higher ASL-signal can be obtained using scenario-(i) due to high FA. The downside of bSSFP sequence is, however, its sensitivity to off-resonance, which causes signal-loss not only in regions of strong field inhomogeneity, but also in downstream vessels (Fig. 8 of Okell et al.[32]). Therefore, scanning should be performed using short TR to minimize phase accrual between excitation pulses, and better performances

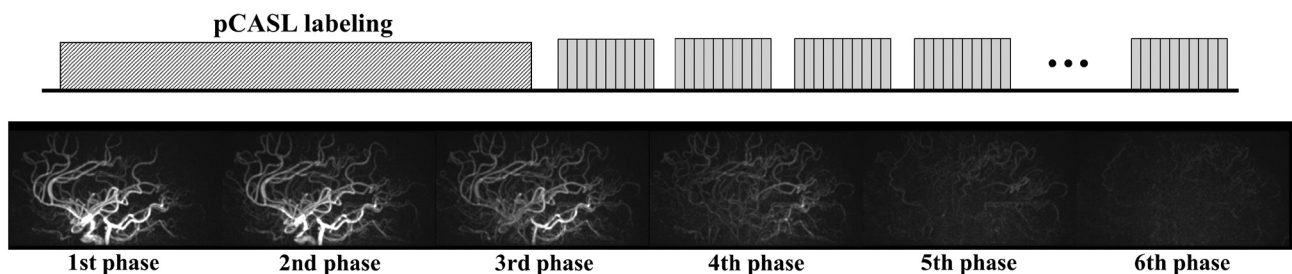can be expected at lower field strength due to less severe B_0 inhomogeneities.

Labeling Module (General)

Arterial spin labeling technique can be divided into three major categories by the means of the labeling mechanism: pulsed ASL (PASL), pseudo-continuous ASL (pCASL) and velocity-selective (VS) ASL. In PASL, as its name implies, a single RF-pulse inverts all spins within a large area as determined by the profile of the RF-pulse (typically 10–20 cm thick slab located proximal to the imaging volume). Such an inversion pulse inverts all spins regardless of its condition, i.e. whether the spins are flowing or static. The typical duration of the labeling RF-pulse is 5–20 ms, which allows depicting the inflow of the labeled arterial blood into the intracranial vascular tree when the readout is started shortly after the labeling pulse (Fig. 5a). Although there are several elaborate PASL techniques designed for

a) PASL Look-Locker

PASL labeling

1st phase   2nd phase   3rd phase   4th phase   5th phase   6th phase

b) pCASL Look-Locker

pCASL labeling

1st phase   2nd phase   3rd phase   4th phase   5th phase   6th phase

c) pCASL Inflow-subtraction

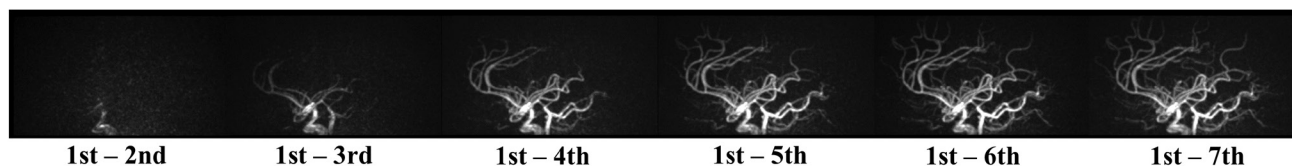1st – 2nd   1st – 3rd   1st – 4th   1st – 5th   1st – 6th   1st – 7th

Fig. 5 Simplified sequence diagrams and typical subtracted MRA images obtained using (**a**) PASL Look-Locker and (**b**) pCASL Look-Locker. (**c**) To enable the visualization of the early inflow phase using pCASL data, inflow subtraction was proposed previously.[24,32] MRA, magnetic resonance angiography; PASL, pulsed arterial spin labeling; pCASL, pseudo-continuous arterial spin labeling.

accurate CBF quantification in perfusion imaging, i.e. QUIPSS II[34] and Q2TIPS,[35] for conventional dynamic MRA (i.e. qualitative visualization of arterial vessels), a simple module with a single labeling pulse such as 'signal targeting with alternating radiofrequency' (STAR)[36,37] and 'flow-sensitive alternating inversion recovery' (FAIR)[38] is sufficient.

In CASL, a long and continuous RF-wave is applied for 1–3 s with a very thin effective labeling plane. The mechanism of labeling is based upon flow-driven adiabatic inversion, in which only the magnetization of the spins flowing through the labeling plane achieve the inversion. In recent years, pCASL[39] has been used more widely than CASL, in which the long continuous RF-wave of CASL is replaced by a train of very short RF-pulses (with typical duration of about 0.5 ms). pCASL labeling brought benefits of easier implementation on clinical MRI scanners and higher labeling efficiency than the conventional CASL.

In PASL, the temporal width of the labeling bolus is determined by the thickness of the labeling pulse, which is limited by the RF-transmit coverage. In contrast, pCASL allows the generation of more labeled arterial blood by applying the labeling for a long duration. This wider temporal width generated by pCASL is very advantageous for perfusion imaging, in which the larger amount of labeled blood directly translates to more accumulation of labeled spins in the brain tissue and thus a higher SNR. Therefore, pCASL is advocated by the above-mentioned consensus statement[9] for ASL perfusion imaging. Also, a previous study in 3D ASL-MRA has shown that substantially higher arterial signal was obtained by pCASL than PASL.[40] However, a dilemma shows up when using pCASL for dynamic MRA: because of its long labeling duration, the earliest labeled blood has already reached the distal arteries even for the first phase acquired immediately after the end of the labeling, thereby making it difficult to depict the early inflow phases (Fig. 5b), which are easily depicted by PASL. As a solution, inflow subtraction was proposed previously,[24,32] in which the second and subsequent phases of the dynamic MRA (subtracted) is further subtracted from the first phase (Fig. 5c). It should be noted, however, that only the labeled blood depicted in the first phase will be visualized, which means that arteries with (very) late arrival (i.e. the label has not arrived by the first phase) will not be visualized even though the labeled blood will reach these distal segments in later phases. Several options could avoid such missed depiction of distal arteries, for example: (i) use very long labeling to make sure the labeled blood has reached the targeted distal arteries (e.g. 3 seconds[24]), (ii) evaluate both the images generated by the conventional subtraction (Fig. 5b) as well as those created by inflow-subtraction (Fig. 5c), (iii) extend the inflow-subtraction using all phases as the reference image.[31] However, none of these three options should be considered to provide a perfect solution, which explains why PASL is still considered as one of preferred labeling techniques for

dynamic ASL-MRA, and has proved its clinical usefulness in several previous clinical studies.[2–5]

When imaging static 3D-MRA, however, the above-mentioned dilemma is no longer relevant, and long pCASL labeling duration will ensures visualization of the complete arterial trees from proximal to distal vessels with adequate SNR.[16,25,27] Moreover, a hybrid of pCASL and PASL was suggested when using large FOV for imaging of extracranial carotid arteries, which could also minimize disappearance of the arterial signal due to fresh unlabeled blood flowing into the imaging volume.[41]

Velocity-selective Labeling

In contrast to the labeling of PASL and pCASL which are based upon spatially selective labeling (i.e. labeling the upstream arterial blood and only flowing blood will move from the labeling location into the imaging volume), the labeling in VS-ASL[42] is based upon velocity: spins flowing above a predefined cut-off velocity are saturated, whereas static tissue remains untouched. Saturation of flowing spins is achieved by a sequence module consisting of non-selective 90°, 180°, 180, −90° pulses in combined with velocity-encoding bipolar-gradients around the 180°-pulses. This labeling module restores the magnetization of non-moving spins from static tissue while moving spins are dephased by the motion-sensitizing gradients, which is very similar to motion-sensitized driven-equilibrium (MSDE) preparation used to suppress blood signal from vessels.[43,44] Such flow sensitive labeling enables the labeling of blood spins within the imaging volume, i.e. label is created much closer to the capillaries, thereby making perfusion measurements less sensitive to arterial transit time differences. Also, for MRA, better visualization of peripheral arteries can be expected as compared with TOF-MRA which often suffers from poor visualization of peripheral arteries due to the saturation effects especially when slow arterial flow is present.

The drawback of the use of VS-labeling is, however, that both arterial and venous blood (and even cerebrospinal fluid) are labeled as long as they are moving faster than the determined threshold velocity. For perfusion imaging, therefore, an elaborate sequence design is proposed to avoid the signal contribution from the venous blood by means of the following three elements: (i) after the VS-labeling, a delay time of about 1600 ms is inserted before the readout to make sure the labeled arterial blood has reached the capillaries, (ii) another (second) VS-labeling is performed just before the readout, and (iii) this second labeling has the flow-sensitizing gradients for both the labeling and control images. When the second labeling is performed, most of the labeled arterial blood (labeled by the first labeling) will move into the microvascular bed, where the flow velocity is below the threshold velocity of VS-labeling. In contrast, the labeled venous blood flows into larger venous vessels during the delay time, where the flow is expected to be faster than when the venous blood

was labeled by the first labeling. The second labeling will therefore crush the label of venous blood, whereas it will leave most of the labeled arterial blood untouched.

However, this elaborate sequence as designed for perfusion imaging is not applicable to MRA, because it would eliminate the arterial blood signal within arteries as well. Another option to separate the signal of arterial blood from venous blood is by labeling blood spins based upon acceleration and deceleration, while the blood spins flowing with a constant velocity are restored. This would discriminate arterial blood from venous blood, because arterial flow is strongly pulsatile. Such an "acceleration" selective labeling can be achieved by replacing the two pair of bipolar-gradients in VS-labeling module with four unipolar-gradients,[45,46] or alternatively by making the polarity of the second refocusing 180°-pulse negative while keeping the bipolar-gradients.[47] The clinical benefits of acceleration-selective labeling was demonstrated by superior depiction of Moyamoya arteries and collateral arteries[48] and complex flow of AVMs including slow draining flow[49] over TOF-MRA.

In all above-mentioned ASL techniques, i.e. PASL, pCASL and VS-ASL, a subtraction is performed to eliminate the signal from static tissue. Such a subtraction operation could experience artefacts induced by subject's motion. There is an interesting extension of VS-labeling approach that does not require subtraction: VS "excitation", which excites only spins flowing within a defined velocity range, while leaving other spins untouched.[50,51] For MRA, this allows the exclusive excitation of flowing blood spins, thereby enabling elimination of signal from static tissue even without subtraction.[52,53] Such VS-excitation is achieved by Fourier-transform of the B_1-field (a similar idea to the excitation k-space that produces spatially selective excitation[54]), which consists of a train of composite pulses incorporating velocity-sensitive bipolar-gradients and refocusing 180°-pulses. This technique was applied for visualization of arteries in lower extremities,[52] and further optimization was made for immunity to B_0/B_1 inhomogeneities, which results in better visualization of peripheral intracranial arteries than TOF-MRA.[53] In the brain, however, it was found that the flow velocity of peripheral arteries and veins do not differ significantly enough to be clearly separated. Subsequently, a new design of the labeling module exhibiting additional RF-pulses was proposed to achieve separated visualization of the arteries and veins.[55]

Vessel-selective Labeling

As shown in Fig. 2, the exclusive visualization of the vascular tree originating from a single selected artery can be performed by spatially selective labeling, which can be achieved by both PASL and pCASL, albeit based upon completely different concepts. In PASL, a spatially selective inversion slab is applied to the target artery. This can most easily be achieved by planning the inversion slab parallel to the target artery in the neck in the inferior–superior direction (as an angulated coronal or sagittal slab). In this manner, the labeling slab will cover the target

artery over a large distance, thereby producing a sufficient amount of labeled blood. However, it also implies that the inversion slab will intersect with the imaging volume, because the labeling slab is not spatially limited in the inferior–superior direction. To avoid this intersection causes artefacts on subtracted image, pre- and post-saturation of the imaging volume should be performed. Such vessel-selective labeling approach using PASL was at first designed for perfusion imaging,[56] and many clinical applications were reported, such as the assessment of collateral circulation,[57] and the contribution of the blood flow via external carotid artery (ECA)[58] in patients with steno-occlusive disease. The same selective labeling approach can be used for 4D-MRA,[59] and an application to intracranial AVM patients was reported.[17] The advantage of the use of PASL for vessel-selective labeling is its sharp profile between the labeled and non-labeled area, which can clearly separate the targeted artery from other arteries. However, due to non-selectivity in the inferior–superior direction (except for the limited coverage of the RF-transmit coil), it can frequently result in unwanted inclusion of other non-targeted arteries, for example, due to tortuous vascular anatomy. Also, the separation of the internal carotid artery (ICA) from the ECA is difficult because the labeling slab usually includes the common carotid artery, which feeds both ICA and ECA.

In pCASL, on the other hand, labeling of arterial blood is performed within a thin labeling plane which needs to be planned perpendicular to the flow direction. Therefore, the labeling plane will not be reoriented as done in PASL. Instead, it is achieved by applying additional in-plane gradients (G_{xy}) in between the labeling RF-pulses (Fig. 6).[60] The application of G_{xy} will generate the phase differences in the direction of G_{xy}, which results in a sinusoidal-like pattern of the labeling efficiency. Such in-plane change of the labeling efficiency can be used for vessel-selective labeling without being much bothered by tortuous vascular anatomy outside of the labeling plane. However, it should be noted that the transition between the labeling and control conditions can be very smooth as shown in Fig. 6, which could cause difficulties in the separation of the targeted artery(ies) from other arteries, when they are located close to each other. By looking more into the labeling process, it becomes clear that the transition between the labeling and control condition depends on the pCASL labeling parameters.[61] First, the strength of G_{xy} determines the distance between the center of the labeling and control conditions and needs therefore to be set according to the arterial layout. Second, there are two approaches how to apply G_{xy}: (a) G_{xy} is applied alternately positive and negative (Fig. 6a),[60] or (b) kept in positive without alternation (Fig. 6b)[62]; (a) will be referred to as "bipolar approach" and (b) as "unipolar approach" throughout this article, respectively. The shape of the spatial inversion modulation is influenced by this choice in G_{xy} approach, the strength of the gradient as used during the pCASL labeling (G_{max}), and the strength of the nonzero mean gradient in the z-direction (G_{mean}).[61] Figure 7 shows an example of the optimized shape

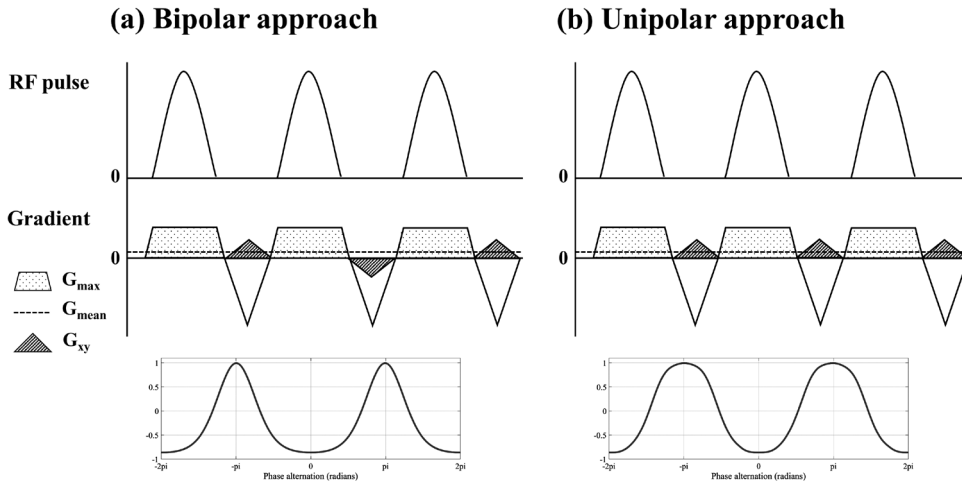## (a) Bipolar approach   (b) Unipolar approach

Fig. 6 Simplified diagrams of vessel-selective pCASL labeling module and examples of the resultant spatial modulation shape of the labeling efficiency: (**a**) "bipolar approach" in which G_{xy} is applied alternately positive and negative, and (**b**) "unipolar approach" in which G_{xy} is kept in positive without alternation.
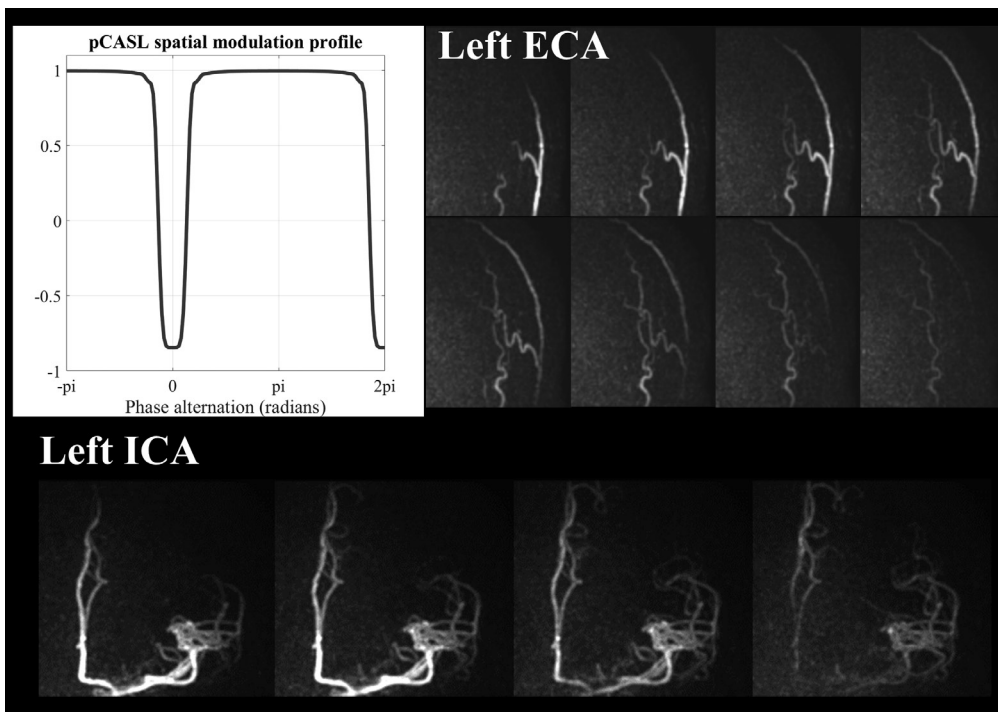

Fig. 7 An example of optimizing the spatial modulation shape of in-plane pCASL labeling efficiency simulated by means of Bloch equation simulations (using parameters used in Suzuki et al.[31]), and 4D-MRA images obtained using this optimized pCASL labeling settings. Arterial trees originating from internal carotid artery (ICA) and external carotid artery (ECA) are clearly separated by a narrow labeling condition in combination with a broader and flatter control condition. pCASL, pseudo-continuous arterial spin labeling.

of the inversion modulation; a steeper transition from the labeling condition to the control condition, and a narrower labeling condition in combination with a broader and flatter control condition were achieved by unipolar approach. Using this optimized settings, clear separation between the ICA and ECA can be achieved (Fig. 7).

The labeling mechanism of pCASL is sensitive to off-resonance, which can result in loss of labeling efficiency.[63,64] Additional shimming and f0-determination at the labeling plane might circumvent such loss in labeling efficiency. It may be worth noting that off-resonance effects are affecting above-mentioned unipolar approach differently compared to the bipolar approach.[62] In the bipolar approach, the inversion of the longitudinal magnetization will be incomplete, i.e. a lower labeling efficiency (Fig. 1A in Wong and Guo[62]). In contrast, off-resonance in the unipolar approach will result in a shift of the inversion profile in the direction of G_{xy} while keeping the similar degree of inversion (Fig. 1B in Wong and Guo[62]). Although such shifted inversion will not affect the maximally achieved labeling efficiency, it could cause labeling of the wrong artery. In both cases, therefore, very good shimming of the labeling plane is essential to gurantee a reliable image quality.

Furthermore, vessel-selective pCASL can be extended to a focal labeling spot that can target a very single artery, rather than the conventional rectangular-like inversion band. Such

a labeling spot can be achieved by rotating the effective direction of G_{xy} pseudo-randomly,[65] or by rotating the direction of G_{xy} in combination with an amplitude modulation of G_{xy}.[66] Using such a "rotating" G_{xy}, the flowing spins are inverted only at the center of G_{xy} rotation, where the additional phase accrual produced by G_{xy} remains close to zero over the labeling period. By adapting the phase of the pCASL RF-pulses, the location of the labeling spot can be controlled. Such a focal labeling spot enables selective labeling of an intracranial artery, even above the Circle of Willis.[16,67]

When multiple arteries need to be labeled consecutively, e.g. the right-ICA (RICA), left-ICA (LICA) and vertebrobasilar arteries (VAs), pairwise acquisitions of labeling/control conditions for each artery would require six acquisitions, which takes considerable scan-time. To address this issue, several time-efficient approaches have been proposed. For example, a single control image can be shared by three labeling images of RICA, LICA and VAs, which reduces the scan-time by two-third of the original pairwise acquisition.[68,69] Alternatively, dual-vessel labeling scheme can also shorten the scan-time by two-third by labeling two arteries simultaneously as follows[70]: (i) LICA + VAs and (ii) RICA + VAs (pairwise labeling/control acquisition). After a subtraction is performed between the labeling and control images for each acquisition of (i) and (ii), arterial signal from either of RICA and LICA can be isolated by assigning ASL-signal present in both acquisitions (i) and (ii) as arterial blood originating from VAs. A theoretical issue with this approach is that mixed blood coming from both ICAs will be misinterpreted as blood from VAs.

Such misinterpretation can be avoided using vessel-encoded (ve)-ASL, in which the labeling patterns are played-out according to a Hadamard-matrix.[60,71] For example, the labeling pattern of four Hadamard-encodings which separates RICA, LICA and VAs from static tissue signal is as follows (Equation [1]):

$$y = \begin{pmatrix} -1 & 1 & 1 & 1 \\ 1 & -1 & 1 & 1 \\ 1 & 1 & -1 & 1 \\ -1 & -1 & -1 & 1 \end{pmatrix} \begin{pmatrix} \mathrm{RICA} \\ \mathrm{LICA} \\ \mathrm{VAs} \\ S \end{pmatrix} \qquad [1]$$

where y is the measured signal and S is static tissue. Each arterial tree arising from RICA, LICA and VAs is calculated by applying the pseudo-inverse matrix of Equation [1]. Very conveniently when applying this approach to perfusion imaging, the multiple vessel-encoding acquisition can be performed as a replacement of signal averaging, which means vessel-selective perfusion imaging can be obtained without extra scan-time or loss in SNR as compared with non-vessel-selective perfusion imaging. In ASL-MRA, however, the entire scan-time is usually spent to obtain high spatial resolution, without performing signal averaging as done in perfusion imaging. The scan-time will therefore increase by the number of Hadamard-encodings divided by two. However, when compared with the traditional one-by-one

acquisition, ve-pCASL still results in a scan-time reduction and SNR efficiency.[33] The minimum number of Hadamard-encodings required to separate the three arterial trees of RICA, LICA and VAs is four as shown in Equation [1]. For successful application of ve-pCASL for ASL-MRA, it is essential to have (i) a sharp spatial transition between the labeling and control conditions to accurately separate the targeted artery from other non-targeted arteries (−1 versus 1 in Equation [1]), and (ii) a broad and flat control condition to provide the same control condition for all non-targeted arteries (1 for all non-targeted arteries in Equation [1]) even though they are located separately. This is important to avoid partial labeling which would cause subtraction artefacts in the reconstructed images, as well as achieve high SNR-efficiency. In our previous study,[61] ve-pCASL 4D-MRA using four Hadamard-encodings resulted in better suppression of non-targeted arteries after the optimization of the spatial inversion modulation, as described earlier in this section and with an example in Fig. 7.

Scan-time

While ASL-based 4D-MRA is flexible to achieve both high spatial and temporal resolution, as mentioned above, the scan-time tends to be relatively long. In previously reported studies of non-vessel-selective 4D-MRA, the mean scan-time was approximately 6:45 min (ranging 5–8.5 min),[1,2,4,22,24,26,27] which is sometimes too long to be included into clinical examinations. This long scan-time can be partly attributed to the fact that, in Look-Locker 4D-ASL, all phases for not only labeling image but also control image are acquired as shown in Fig. 8a. A recently developed technique, 'Acquisition of control and labeled image in the same shot' (ACTRESS) shortens the scan-time of Look-Locker 4D-MRA by avoiding the acquisition of complete Look-Locker cycles for control image.[30] Instead, in ACTRESS as Fig. 8b shows, a single control image is acquired before applying the labeling pulse, which is followed by traditional Look-Locker readout that acquires labeled images at multiple TIs. Subsequently, all labeled images are subtracted from the single control image, thereby providing 4D-MRA images with similar image quality to traditional 4D-MRA even though the scan-time is nearly half (Fig. 9). It should be noted that the ACTRESS approach is specifically designed for 4D-MRA and could not be applied to quantitative perfusion imaging. When applied to perfusion imaging, ACTRESS would not lead to complete elimination of the background signal from the static tissue, because of slightly different MT-effects for the control image and the labeling images at multiple TIs. For 4D-MRA, however, such residual signal from the static tissue is very minor compared with the high intravascular ASL-signal, and does not hinder visualization of arteries. Although this ACTRESS approach was designed for non-vessel-selective 4D-MRA using PASL, it can be also extended to vessel-selective 4D-MRA using pCASL.[31]

Undersampled 3D radial acquisition technique is an another option to shorten the scan-time. In fact, ASL-based
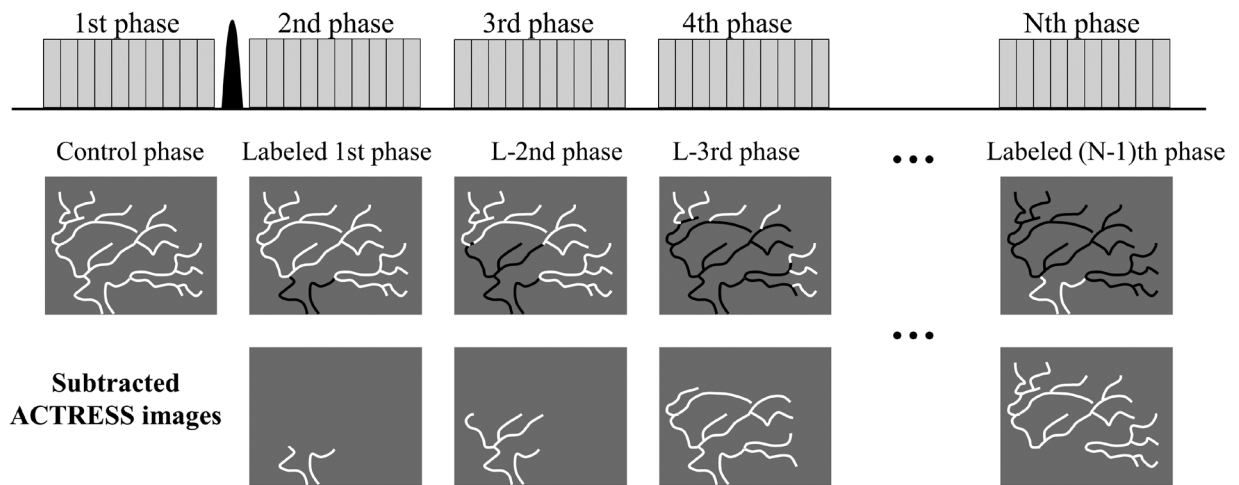
a) Traditional Look-Locker ASL
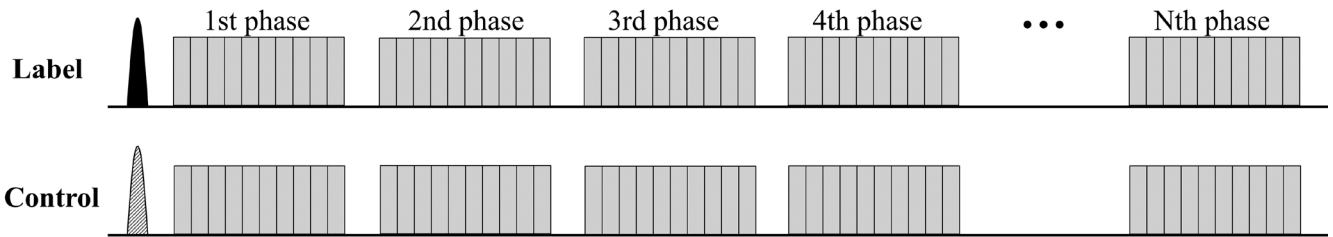
b) ACTRESS approach

Fig. 8 Simplified diagrams of (**a**) traditional PASL with Look-Locker readout, and (**b**) 'acquisition of control and labeled images in the same shot' (ACTRESS) approach. The labeled and unlabeled blood are illustrated in black and white, respectively. PASL, pulsed arterial spin labeling.

angiography is very suitable for undersampling combined with radial acquisition: because of the high sparsity of ASL-based angiographic images [i.e. only small number of pixels have bright signal, while other pixels are (ideally) zero], the artefacts that appear as a result of undersampling behave like diffusive background noise that does not really affect image quality, thereby allowing high undersampling factors and shorter scan-time suitable for clinical examinations.[25] Also, radial acquisition with a Golden-ratio angle increment has been suggested as an optimized sampling order for 4D-MRA. With this sampling scheme, subsequent radial lines are acquired with a constant azimuthal increment based on the Golden-ratio increment of 111.25°,[72] which ensures that any combination of consecutively acquired spokes will result in a homogeneous filling of *k*-space. This allows flexible reconstruction approaches such as sliding-window[73] and '*k*-space weighted image contrast' (KWIC)[74] to achieve high temporal resolution.

Additionally, compressed-sensing reconstruction will benefit from the sparsity of ASL-MRA and allows acquisition of images with high spatial and temporal resolution within a short scan-time, while avoiding the typical temporal smoothness observed when using techniques such as view-sharing and KWIC reconstruction.[75]

Combined Acquisition of 4D-MRA and Perfusion Image

As mentioned earlier, for 4D-MRA and perfusion imaging, the optimal timing of the readout (i.e. TI/PLD) usually differs: in perfusion imaging, a long enough TI/PLD needs to be chosen so that all (or at least most of) the labeled blood has reached the brain tissue and little signal arises from arteries. In 4D-MRA, on the other hand, the readout is started shortly after the labeling and repeated several times using Look-Locker readout to dynamically visualize the inflow of labeled blood into the arterial tree. These differences suggest something very interesting: during the long PLD of perfusion imaging, 4D-MRA can be acquired, while both acquisitions exploit the same label as generated by a single labeling module. However, there are three major challenges that make such approach difficult. First, the desired spatial resolution of 4D-MRA and perfusion imaging are very different. Second, the optimal labeling duration is different: for perfusion
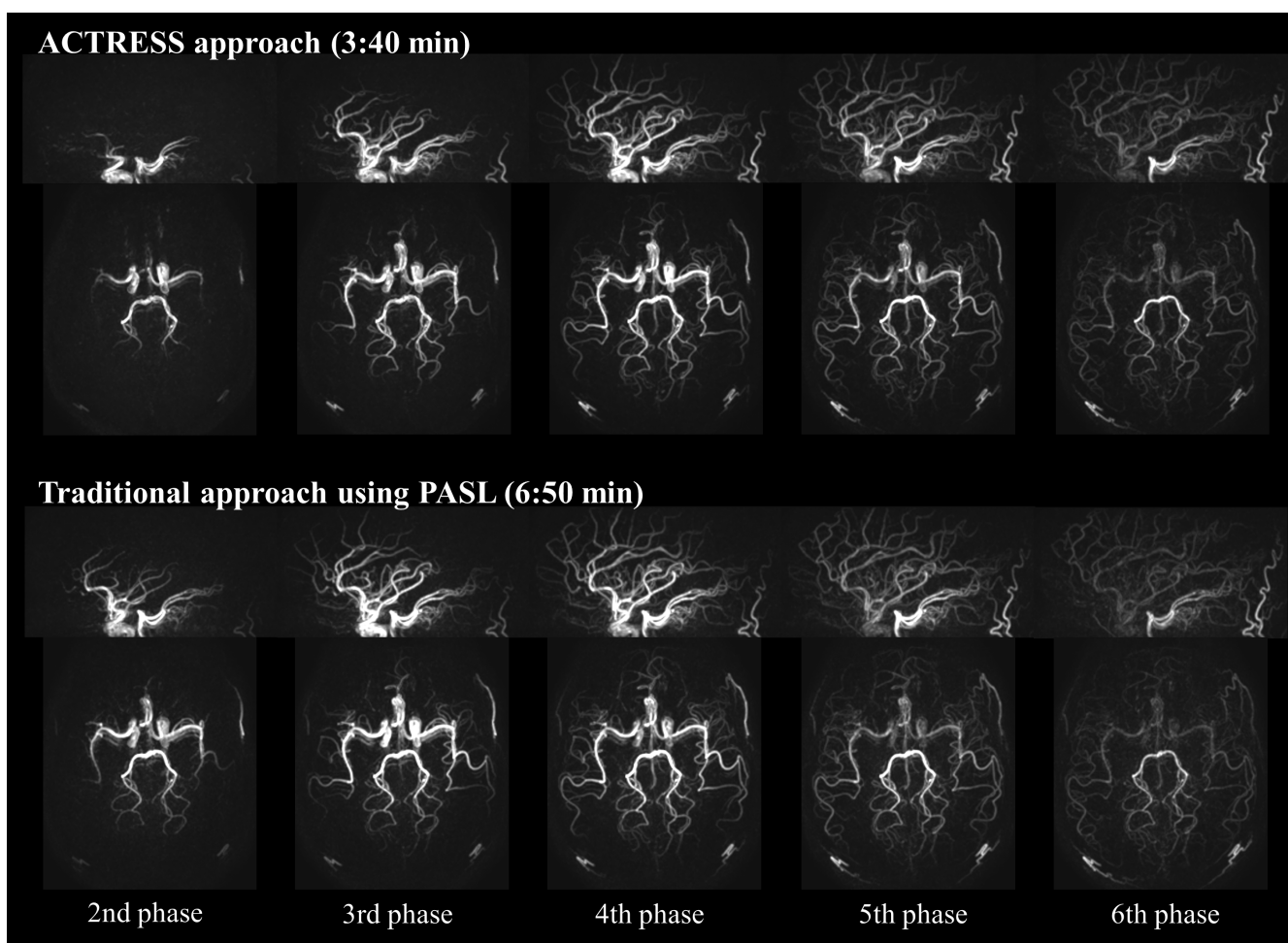
Fig. 9 An example comparison of the traditional 4D-MRA obtained using the STAR sequence and ACTRESS 4D-MRA. MRA, magnetic resonance angiography; STAR, signal targeting with alternating radiofrequency; ACTRESS, acquisition of control and labeled image in the same shot.

image, a labeling duration of approximately 1.8 s is advised to obtain sufficient SNR (as recommended by the white-paper[9]). Such a long labeling duration would, however, already fill up almost the complete arterial tree, and spoil the opportunity to depict the labeled blood flowing into the vascular tree by 4D-MRA. At last but not least, when 4D-MRA is acquired by Look-Locker readout, the longitudinal magnetization of the labeled blood will be consumed too much due to the repetitive excitation RF-pulses, therefore, the SNR of the perfusion image acquired after 4D-MRA will be barely sufficient for clinical use.

Two interesting approaches have been proposed that achieve combined acquisition of 4D-MRA and perfusion imaging by addressing those challenges. The first approach[76] proposed to use time-encoded (te)-pCASL,[77] in which images with multiple delays (e.g. N) are obtained by dividing the long pCASL labeling train into N-segments (sub-boli) which condition (label/control) varies according to $(N + 1)$ Hadamard-matrix. Using an appropriate decoding step, only the ASL-signal from a single sub-bolus can be reconstructed

and N-images with different PLD can be obtained. The benefit of using te-pCASL for combined acquisition of 4D-MRA and perfusion imaging is twofold. First, multi-PLD images can be obtained without relying on Look-Locker readout, thereby largely alleviating the above-mentioned third challenge. Second, a sub-bolus with long labeling duration and PLD for perfusion imaging and several sub-boli with short labeling duration for dynamic MRA can be implemented into a single labeling module, which solves the second challenge. To solve the first challenge, in this study, a 3D-TFEPI sequence with high spatial resolution for MRA is immediately followed by multi-slice single-shot EPI sequence with low spatial resolution for perfusion imaging using a special setup. Figure 10 shows that perfusion image was successfully acquired after the acquisition of 4D-MRA, which also shows asymmetrical arrival of the labeled blood.

In the second approach,[73] a radial acquisition with a Golden-ratio angle increment was employed by taking the advantages of its good compatibility with ASL-MRA and the capability of flexible temporal and spatial reconstruction, as
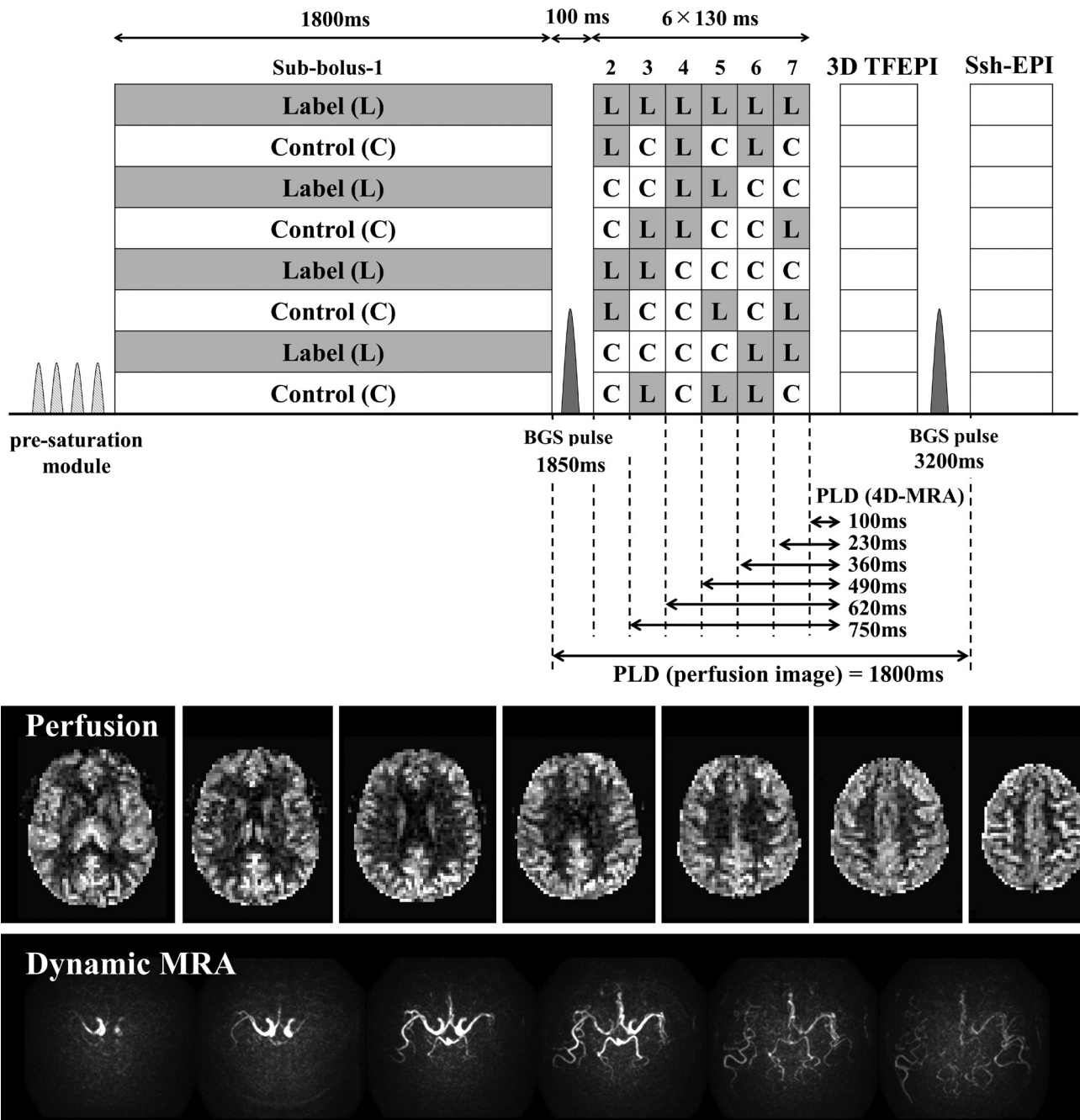
	1800ms		100 ms	6 × 130 ms								
	Sub-bolus-1			2	3	4	5	6	7	3D TFEPI	Ssh-EPI
	Label (L)			L	L	L	L	L	L		
	Control (C)			L	C	L	C	L	C		
	Label (L)			C	C	L	L	C	C		
	Control (C)			C	L	L	C	C	L		
	Label (L)			L	L	C	C	C	C		
	Control (C)			L	C	C	L	C	L		
	Label (L)			C	C	C	C	L	L		
	Control (C)			C	L	C	L	L	C		

pre-saturation module

BGS pulse 1850ms

BGS pulse 3200ms

PLD (4D-MRA)
100ms
230ms
360ms
490ms
620ms
750ms

PLD (perfusion image) = 1800ms

Perfusion

Dynamic MRA

Fig. 10 A sequence diagram of the simultaneous acquisition of 4D-MRA and perfusion image by means of te-pCASL. Example images show that perfusion image was successfully acquired after the acquisition of 4D-MRA, which also shows asymmetrical arrival of the labeled blood. MRA, magnetic resonance angiography; pCASL, (pseudo-)continuous arterial spin labeling.

reviewed in the previous section. High temporal resolution for dynamic-MRA can be achieved by limiting a number of spokes acquired after each labeling. Although the labeling and acquisition can be repeated to obtain more spokes, it would result in longer scan-time. Therefore, the reconstruction of dynamic-MRA has to be performed under highly undersampled conditions. However, as discussed earlier, thanks to the high sparsity of ASL-MRA as well as contrast-to-noise ratio of arterial signal, the expected undersampling

artefacts will not hinder the visualization of arteries. In contrast, perfusion imaging is not very suitable for such high undersampling factors, because the perfusion image is less sparse and the SNR is much lower. However, since the signal change of tissue perfusion is not as dynamic as the one at arteries, the perfusion image can be reconstructed at a much lower temporal resolution using more spokes. Finally, because the spatial resolution can be much lower than for MRA, perfusion image can be generated without relying on
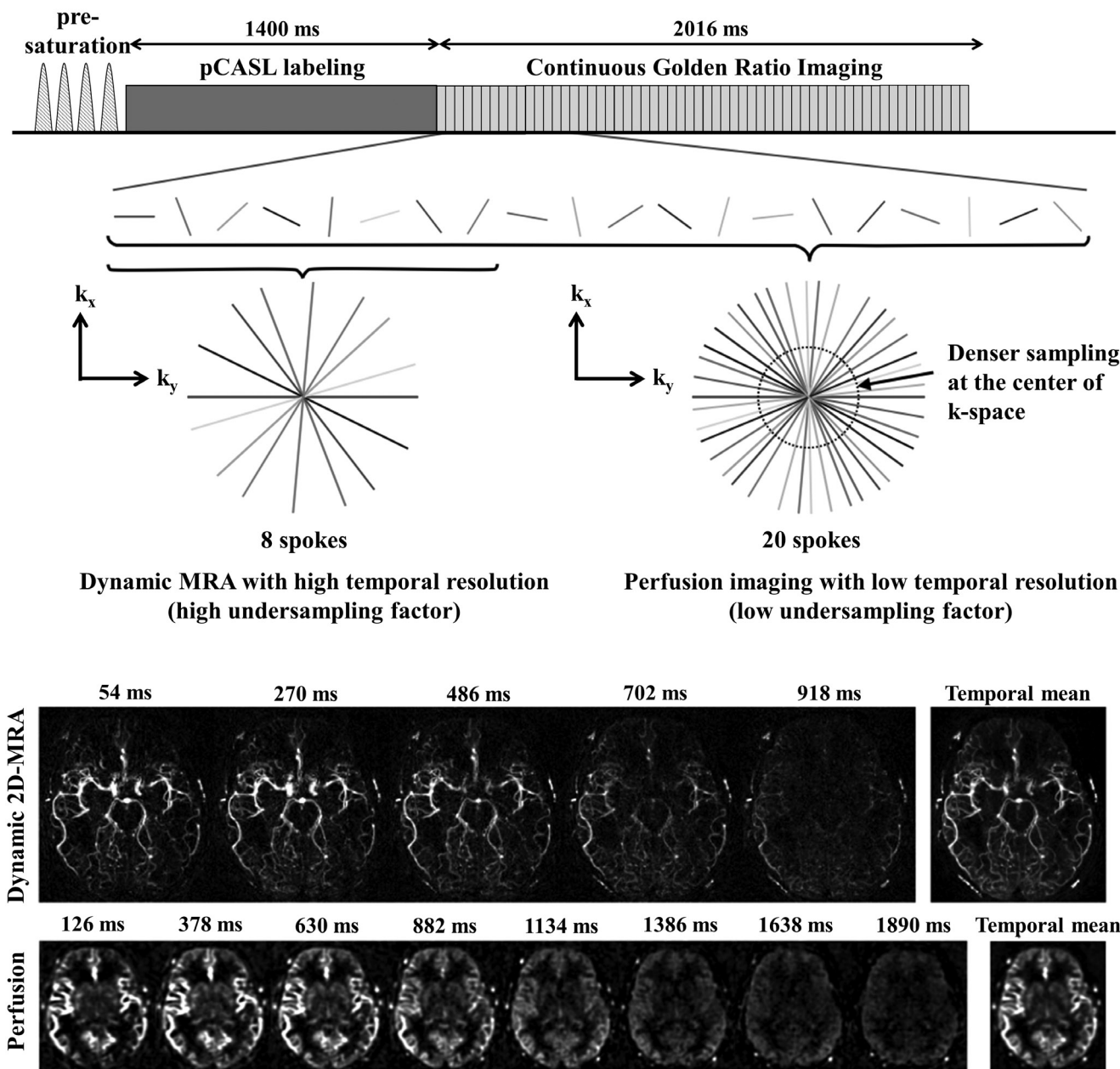
Fig. 11 A sequence diagram of the combined acquisition of angiographic and perfusion image by means of the radial acquisition with a Golden-ratio angle. Example images show temporal changes in angiographic and perfusion images. Image were reproduced from the Okell[73] with permission from Dr. Thomas Okell, University of Oxford.

a high undersampling factor. Figure 11 shows the sequence schema and example dynamic 2D-MRA and perfusion images obtained by this technique. Another interesting advantage of this approach is that the image for dynamic-MRA and perfusion image can be reconstructed retrospectively at arbitrary time point. Such "tailored" reconstruction could be very helpful for patients who have altered flow hemodynamics due to their clinical conditions, such as rapid shunting or slow collateral flow.

Although such a combined acquisition of dynamic-MRA and perfusion image has not been applied to clinical cases

yet, the ability to obtain both macro- and microvascular flow information in a single acquisition would be useful for many cerebrovascular diseases. In a qualitative way, for example, dynamic-MRA could show asymmetrical flow difference caused by mild stenosis at the neck even before intracranial TOF-MRA or the ASL CBF-map (obtained with a single PLD) would depict this. Also, when hyperintensity signal appears on perfusion images after vascular treatment for the steno-occlusive diseases (such as carotid endarterectomy and stenting), the macrovascular flow information could help to distinguish hyperperfusion from residual arterial transit

delay artefacts. Moreover, in a quantitative way, dynamic-MRA could provide macrovascular flow information such as bolus delay and dispersion for more accurate quantitative analysis of perfusion data.

Conclusion

In this article, the implementation and recent developments in ASL-based MRA were discussed, especially by highlighting the differences between ASL-MRA and ASL perfusion imaging. Apart from the fact that ASL does not rely on contrast agent, there are more benefits of using ASL for MRA, e.g. by enabling vessel-specific visualization of the vasculature. Although its clinical use is still limited, we hope this article will encourage the use of ASL-MRA and help the spread into clinical protocols, just as ASL perfusion imaging has been experiencing in the last few years.

Acknowledgments

Conflicts of Interest

MJP van Osch receives grant support from Philips. The other authors have no conflict of interest related to this work.

References

1. Yu S, Yan L, Yao Y, et al. Noncontrast dynamic MRA in intracranial arteriovenous malformation (AVM), comparison with time of flight (TOF) and digital subtraction angiography (DSA). Magn Reson Imaging 2012; 30:869–877.
2. Iryo Y, Hirai T, Kai Y, et al. Intracranial dural arteriovenous fistulas: evaluation with 3-T four-dimensional MR angiography using arterial spin labeling. Radiology 2014; 271:193–199.
3. Iryo Y, Hirai T, Nakamura M, et al. Collateral circulation via the circle of Willis in patients with carotid artery steno-occlusive disease: evaluation on 3-T 4D MRA using arterial spin labelling. Clin Radiol 2015; 70:960–965.
4. Uchino H, Ito M, Fujima N, et al. A novel application of four-dimensional magnetic resonance angiography using an arterial spin labeling technique for noninvasive diagnosis of Moyamoya disease. Clin Neurol Neurosurg 2015; 137:105–111.
5. Hu HH, Pokorney AL, Stefani N, Chia JM, Miller JH. Non-gadolinium dynamic angiography of the neurovasculature using arterial spin labeling MRI: preliminary experience in children. MAGMA 2017; 30:107–112.
6. Golay X, Guenther M. Arterial spin labelling: final steps to make it a clinical reality. MAGMA 2012; 25:79–82.
7. Grade M, Hernandez Tamames JA, Pizzini FB, Achten E, Golay X, Smits M. A neuroradiologist's guide to arterial spin labeling MRI in clinical practice. Neuroradiology 2015; 57:1181–1202.
8. Gulani V, Calamante F, Shellock FG, Kanal E, Reeder SB; International Society for Magnetic Resonance in Medicine. Gadolinium deposition in the brain: summary of evidence and recommendations. Lancet Neurol 2017; 16:564–570.
9. Alsop DC, Detre JA, Golay X, et al. Recommended implementation of arterial spin-labeled perfusion MRI for clinical applications: a consensus of the ISMRM perfusion study group and the European consortium for ASL in dementia. Magn Reson Med 2015; 73:102–116.
10. Cashen TA, Jeong H, Shah MK, et al. 4D radial contrast-enhanced MR angiography with sliding subtraction. Magn Reson Med 2007; 58:962–972.
11. Jeong HJ, Cashen TA, Hurley MC, et al. Radial sliding-window magnetic resonance angiography (MRA) with highly-constrained projection reconstruction (HYPR). Magn Reson Med 2009; 61:1103–1113.
12. Eddleman CS, Jeong HJ, Hurley MC, et al. 4D radial acquisition contrast-enhanced MR angiography and intracranial arteriovenous malformations: quickly approaching digital subtraction angiography. Stroke 2009; 40:2749–2753.
13. Velikina JV, Johnson KM, Wu Y, Samsonov AA, Turski P, Mistretta CA. PC HYPR flow: a technique for rapid imaging of contrast dynamics. J Magn Reson Imaging 2010; 31:447–456.
14. Rapacchi S, Natsuaki Y, Plotnik A, et al. Reducing view-sharing using compressed sensing in time-resolved contrast-enhanced magnetic resonance angiography. Magn Reson Med 2015; 74:474–481.
15. Wu Y, Kim N, Korosec FR, et al. 3D time-resolved contrast-enhanced cerebrovascular MR angiography with subsecond frame update times using radial *k*-space trajectories and highly constrained projection reconstruction. AJNR Am J Neuroradiol 2007; 28:2001–2004.
16. Jensen-Kondering U, Lindner T, van Osch MJ, Rohr A, Jansen O, Helle M. Superselective pseudo-continuous arterial spin labeling angiography. Eur J Radiol 2015; 84:1758–1767.
17. Fujima N, Osanai T, Shimizu Y, et al. Utility of noncontrast-enhanced time-resolved four-dimensional MR angiography with a vessel-selective technique for intracranial arteriovenous malformations. J Magn Reson Imaging 2016; 44:834–845.
18. Jezzard P, Chappell MA, Okell TW. Arterial spin labeling for the measurement of cerebral perfusion and angiography. J Cereb Blood Flow Metab 2018; 38:603–626.
19. Hernandez-Garcia L, Lahiri A, Schollenberger J. Recent progress in ASL. Neuroimage 2019; 187:3–16.
20. van Osch MJ, Teeuwisse WM, Chen Z, Suzuki Y, Helle M, Schmid S. Advances in arterial spin labelling MRI methods for measuring perfusion and collateral flow. J Cereb Blood Flow Metab 2018; 38:1461–1480.
21. Wong EC. An introduction to ASL labeling techniques. J Magn Reson Imaging 2014; 40:1–10.

22. Yan L, Salamon N, Wang DJ. Time-resolved noncontrast enhanced 4-D dynamic magnetic resonance angiography using multibolus TrueFISP-based spin tagging with alternating radiofrequency (TrueSTAR). Magn Reson Med 2014; 71:551–560.

23. Shao X, Zhao Z, Russin J, et al. Quantification of intracranial arterial blood flow using noncontrast enhanced 4D dynamic MR angiography. Magn Reson Med 2019; 82:449–459.

24. Kopeinigg D, Bammer R. Time-resolved angiography using inflow subtraction (TRAILS). Magn Reson Med 2014; 72:669–678.

25. Wu H, Block WF, Turski PA, Mistretta CA, Johnson KM. Noncontrast-enhanced three-dimensional (3D) intracranial MR angiography using pseudocontinuous arterial spin labeling and accelerated 3D radial acquisition. Magn Reson Med 2013; 69:708–715.

26. Wu H, Block WF, Turski PA, et al. Noncontrast dynamic 3D intracranial MR angiography using pseudo-continuous arterial spin labeling (PCASL) and accelerated 3D radial acquisition. J Magn Reson Imaging 2014; 39:1320–1326.

27. Schubert T, Clark Z, Sandoval-Garcia C, et al. Non contrast, pseudo-continuous arterial spin labeling and accelerated 3-dimensional radial acquisition intracranial 3-dimensional magnetic resonance angiography for the detection and classification of intracranial arteriovenous shunts. Invest Radiol 2018; 53:80–86.

28. Günther M, Bock M, Schad LR. Arterial spin labeling in combination with a look-locker sampling strategy: inflow turbo-sampling EPI-FAIR (ITS-FAIR). Magn Reson Med 2001; 46:974–984.

29. Wielopolski PA, Adamis M, Prasad P, Gaa J, Edelman R. Breath-hold 3D STAR MR angiography of the renal arteries using segmented echo planar imaging. Magn Reson Med 1995; 33:432–438.

30. Suzuki Y, Fujima N, Ogino T, et al. Acceleration of ASL-based time-resolved MR angiography by acquisition of control and labeled images in the same shot (ACTRESS). Magn Reson Med 2018; 79:224–233.

31. Suzuki Y, Okell TW, Fujima N, van Osch MJP. Acceleration of vessel-selective dynamic MR angiography by pseudocontinuous arterial spin labeling in combination with Acquisition of ConTRol and labEled images in the Same Shot (ACTRESS). Magn Reson Med 2019; 81:2995–3006.

32. Okell TW, Schmitt P, Bi X, et al. Optimization of 4D vessel-selective arterial spin labeling angiography using balanced steady-state free precession and vessel-encoding. NMR Biomed 2016; 29:776–786.

33. Okell TW, Garcia M, Chappell MA, Byrne JV, Jezzard P. Visualizing artery-specific blood flow patterns above the circle of Willis with vessel-encoded arterial spin labeling. Magn Reson Med 2019; 81:1595–1604.

34. Wong EC, Buxton RB, Frank LR. Quantitative imaging of perfusion using a single subtraction (QUIPSS and QUIPSS II). Magn Reson Med 1998; 39:702–708.

35. Luh WM, Wong EC, Bandettini PA, Hyde JS. QUIPSS II with thin-slice TI1 periodic saturation: a method for improving accuracy of quantitative perfusion imaging using pulsed arterial spin labeling. Magn Reson Med 1999; 41:1246–1254.

36. Edelman RR, Siewert B, Adamis M, Gaa J, Laub G, Wielopolski P. Signal targeting with alternating radiofrequency (STAR) sequences: application to MR angiography. Magn Reson Med 1994; 31:233–238.

37. Edelman RR, Siewert B, Darby DG, et al. Qualitative mapping of cerebral blood flow and functional localization with echo-planar MR imaging and signal targeting with alternating radio frequency. Radiology 1994; 192:513–520.

38. Kim SG. Quantification of relative cerebral blood flow change by flow-sensitive alternating inversion recovery (FAIR) technique: application to functional mapping. Magn Reson Med 1995; 34:293–301.

39. Dai W, Garcia D, de Bazelaire C, Alsop DC. Continuous flow-driven inversion for arterial spin labeling using pulsed radio frequency and gradient fields. Magn Reson Med 2008; 60:1488–1497.

40. Koktzoglou I, Gupta N, Edelman RR. Nonenhanced extracranial carotid MR angiography using arterial spin labeling: improved performance with pseudocontinuous tagging. J Magn Reson Imaging 2011; 34:384–394.

41. Koktzoglou I, Meyer JR, Ankenbrandt WJ, et al. Nonenhanced arterial spin labeled carotid MR angiography using three-dimensional radial balanced steady-state free precession imaging. J Magn Reson Imaging 2015; 41:1150–1156.

42. Wong EC, Cronin M, Wu WC, Inglis B, Frank LR, Liu TT. Velocity-selective arterial spin labeling. Magn Reson Med 2006; 55:1334–1341.

43. Wang J, Yarnykh VL, Hatsukami T, Chu B, Balu N, Yuan C. Improved suppression of plaque-mimicking artifacts in black-blood carotid atherosclerosis imaging using a multislice motion-sensitized driven-equilibrium (MSDE) turbo spin-echo (TSE) sequence. Magn Reson Med 2007; 58:973–981.

44. Wang J, Yarnykh VL, Yuan C. Enhanced image quality in black-blood MRI using the improved motion-sensitized driven-equilibrium (iMSDE) sequence. J Magn Reson Imaging 2010; 31:1256–1263.

45. Priest AN, Taviani V, Graves MJ, Lomas DJ. Improved artery-vein separation with acceleration-dependent preparation for non-contrast-enhanced magnetic resonance angiography. Magn Reson Med 2014; 72:699–706.

46. Schmid S, Ghariq E, Teeuwisse WM, Webb A, van Osch MJ. Acceleration-selective arterial spin labeling. Magn Reson Med 2014; 71:191–199.

47. Obara M, Togao O, Yoneyama M, et al. Acceleration-selective arterial spin labeling for intracranial MR angiography with improved visualization of cortical arteries and suppression of cortical veins. Magn Reson Med 2017; 77:1996–2004.

48. Togao O, Hiwatashi A, Obara M, et al. Acceleration-selective arterial spin-labeling MR angiography used to visualize distal cerebral arteries and collateral vessels in moyamoya disease. Radiology 2018; 286:611–621.

49. Togao O, Hiwatashi A, Yamashita K, et al. Acceleration-selective arterial spin labeling MR angiography for visualization of brain arteriovenous malformations. Neuroradiology 2019; 61:979–989.

50. Norris DG, Schwarzbauer C. Velocity selective radiofrequency pulse trains. J Magn Reson 1999; 137:231–236.

51. de Rochefort L, Maître X, Bittoun J, Durand E. Velocity-selective RF pulses in MRI. Magn Reson Med 2006; 55:171–176.

52. Shin T, Hu BS, Nishimura DG. Off-resonance-robust velocity-selective magnetization preparation for non-contrast-enhanced peripheral MR angiography. Magn Reson Med 2013; 70:1229–1240.

53. Qin Q, Shin T, Schär M, Guo H, Chen HW, Qiao Y. Velocity-selective magnetization-prepared non-contrast-enhanced cerebral MR angiography at 3 Tesla: improved immunity to B0/B1 inhomogeneity. Magn Reson Med 2016; 75:1232–1241.

54. Pauly J, Nishimura D, Macovski A. A *k*-space analysis of small-tip-angle excitation. 1989. J Magn Reson 2011; 213:544–557.

55. Li W, Xu F, Schär M, et al. Whole-brain arteriography and venography: using improved velocity-selective saturation pulse trains. Magn Reson Med 2018; 79:2014–2023.

56. Golay X, Petersen ET, Hui F. Pulsed star labeling of arterial regions (PULSAR): a robust regional perfusion technique for high field imaging. Magn Reson Med 2005; 53:15–21.

57. Chng SM, Petersen ET, Zimine I, Sitoh YY, Lim CC, Golay X. Territorial arterial spin labeling in the assessment of collateral circulation: comparison with digital subtraction angiography. Stroke 2008; 39:3248–3254.

58. van Laar PJ, van der Grond J, Bremmer JP, Klijn CJ, Hendrikse J. Assessment of the contribution of the external carotid artery to brain perfusion in patients with internal carotid artery occlusion. Stroke 2008; 39:3003–3008.

59. Nakamura M, Yoneyama M, Tabuchi T, et al. Vessel-selective, non-contrast enhanced, time-resolved MR angiography with vessel-selective arterial spin labeling technique (CINEMA-SELECT) in intracranial arteries. Radiol Phys Technol 2013; 6:327–334.

60. Wong EC. Vessel-encoded arterial spin-labeling using pseudocontinuous tagging. Magn Reson Med 2007; 58:1086–1091.

61. Suzuki Y, van Osch MJP, Fujima N, Okell TW. Optimization of the spatial modulation function of vessel-encoded pseudocontinuous arterial spin labeling and its application to dynamic angiography. Magn Reson Med 2019; 81:410–423.

62. Wong EC, Guo J. Blind detection of vascular sources and territories using random vessel encoded arterial spin labeling. MAGMA 2012; 25:95–101.

63. Jahanian H, Noll DC, Hernandez-Garcia L. B0 field inhomogeneity considerations in pseudo-continuous arterial spin labeling (pCASL): effects on tagging efficiency and correction strategy. NMR Biomed 2011; 24:1202–1209.

64. Shin DD, Liu TT, Wong EC, Shankaranarayanan A, Jung Y. Pseudocontinuous arterial spin labeling with optimized tagging efficiency. Magn Reson Med 2012; 68:1135–1144.

65. Helle M, Norris DG, Rüfer S, Alfke K, Jansen O, van Osch MJ. Superselective pseudocontinuous arterial spin labeling. Magn Reson Med 2010; 64:777–786.

66. Dai W, Robson PM, Shankaranarayanan A, Alsop DC. Modified pulsed continuous arterial spin labeling for labeling of a single artery. Magn Reson Med 2010; 64:975–982.

67. Helle M, Rüfer S, van Osch MJ, et al. Superselective arterial spin labeling applied for flow territory mapping in various cerebrovascular diseases. J Magn Reson Imaging 2013; 38:496–503.

68. Kamano H, Yoshiura T, Hiwatashi A, et al. Accelerated territorial arterial spin labeling based on shared rotating control acquisition: an observer study for validation. Neuroradiology 2012; 54:65–71.

69. Lindner T, Larsen N, Jansen O, Helle M. Accelerated visualization of selected intracranial arteries by cycled super-selective arterial spin labeling. MAGMA 2016; 29:843–852.

70. Zimine I, Petersen ET, Golay X. Dual vessel arterial spin labeling scheme for regional perfusion imaging. Magn Reson Med 2006; 56:1140–1144.

71. Günther M. Efficient visualization of vascular territories in the human brain by cycled arterial spin labeling MRI. Magn Reson Med 2006; 56:671–675.

72. Winkelmann S, Schaeffter T, Koehler T, Eggers H, Doessel O. An optimal radial profile order based on the Golden Ratio for time-resolved MRI. IEEE Trans Med Imaging 2007; 26:68–76.

73. Okell TW. Combined angiography and perfusion using radial imaging and arterial spin labeling. Magn Reson Med 2019; 81:182–194.

74. Song HK, Yan L, Smith RX, et al. Noncontrast enhanced four-dimensional dynamic MRA with golden angle radial acquisition and K-space weighted image contrast (KWIC) reconstruction. Magn Reson Med 2014; 72:1541–1551.

75. Zhou Z, Han F, Yu S, et al. Accelerated noncontrast-enhanced 4-dimensional intracranial MR angiography using golden-angle stack-of-stars trajectory and compressed sensing with magnitude subtraction. Magn Reson Med 2018; 79:867–878.

76. Suzuki Y, Helle M, Koken P, Van Cauteren M, van Osch MJP. Simultaneous acquisition of perfusion image and dynamic MR angiography using time-encoded pseudo-continuous ASL. Magn Reson Med 2018; 79:2676–2684.

77. Wells JA, Lythgoe MF, Gadian DG, Ordidge RJ, Thomas DL. In vivo Hadamard encoded continuous arterial spin labeling (H-CASL). Magn Reson Med 2010; 63:1111–1118.

78. Lu H, Xu F, Grgac K, Liu P, Qin Q, van Zijl P. Calibration and validation of TRUST MRI for the estimation of cerebral blood oxygenation. Magn Reson Med 2012; 67:42–49.